CrossMark

ORIGINAL ARTICLE

Proposals for risk assessment of major cations in surface water and deep sediment: iso-cation curves, probabilities of occurrence and non-occurrence of cations

Fatih Külahcı[1] (ORCID)

Abstract Spatial analysis and stochastic risk analysis methodologies are proposed for the characterisation of major cations (Mg, Ca, K, Na and Zn) in deep sediments and surface waters of the Keban Reservoir, Turkey. Curves denoted as "iso-cation curves" were drawn using the spatial analysis of the major cations. Spatial diagrams and risk assessment allowed significant conclusions about the nature of the variations in cation concentration in the reservoir. Major cations are measured at 20 different locations within the reservoir, and their comparisons are presented through both spatial distribution and risk analysis models for each ion. Their collective behaviour was also analysed by comparing spatial diagrams of surface water and deep sediment concentrations. Finally, the iso-cation curves and achievement of the occurrence and/or non-occurrence cation probabilities in any research area can be generalised to other the environment sciences. This calculation can be extended easily to cover all pollutants at micro- and macroscales.

Keywords Risk assessment · Risk analysis · Cation · Spatial analysis · Lake

Introduction

The concept of geochemical cycling, or the movement of elements through various parts of the earth, including the atmosphere, is essential to a proper understanding of the overall role of these elements, especially their environmental significance (Swaine 2000).

Concentrations of major cations in the environment are important to the survival of living creatures. On Earth, Mg is the eighth most abundant element and constitutes 2 % of the Earth's crust. Due to its high reactivity, Mg is not found in nature as a metal; instead, it is found in the form of various salts or ionised in water. Mg is needed both in various biological systems and in industrial processes and metallurgy. A higher content of Mg is characteristic of basic and ultra-basic magmatic and metamorphic rocks (e.g. basalt) and their weathering products (Merian et al. 2004a). Mg-rich rock-forming minerals include biotitic and other dark-coloured silicate minerals, as well as serpentine. Ca is enriched in limestone and dolomite in the form of $CaCO_3$ and in lime-free basic silicate rocks, such as basalt. Soils formed in dry regions generally contain larger amounts of calcium than soils in humid regions (Merian et al. 2004a). K makes up 2.6 % of the Earth's crust by weight. This element is enriched in acid magmatic rocks, such as granite, and in clay minerals. In uplifted marine sediments, the Na content may be high, and in igneous rocks, the ratio of K by weight is 0.92. Magmatic rocks contain, on average, 28 g Na kg^{-1}, whereas sedimentary rocks accumulate lower Na concentrations (Merian et al. 2004b). Zn in soil is easily absorbed by mineral and organic substances; it accumulates primarily in the soil surface layer and is fairly uniformly distributed between the following fractions: dissolved in soil water, exchangeable bound to organic ligands, occluded in secondary clay minerals and metal oxides/hydroxides and present in primary minerals (Viets 1962).

Although various chemical elements are found in rocks, their solutions are also abundant in running water. They may therefore accumulate in deep sediments in reservoirs, though the surface water mineral content may be rather different. The difference between the deep sediment and

✉ Fatih Külahcı
fatihkulahci@firat.edu.tr

1 Physics Department, Science Faculty, Fırat University, 23119 Elazig, Turkey
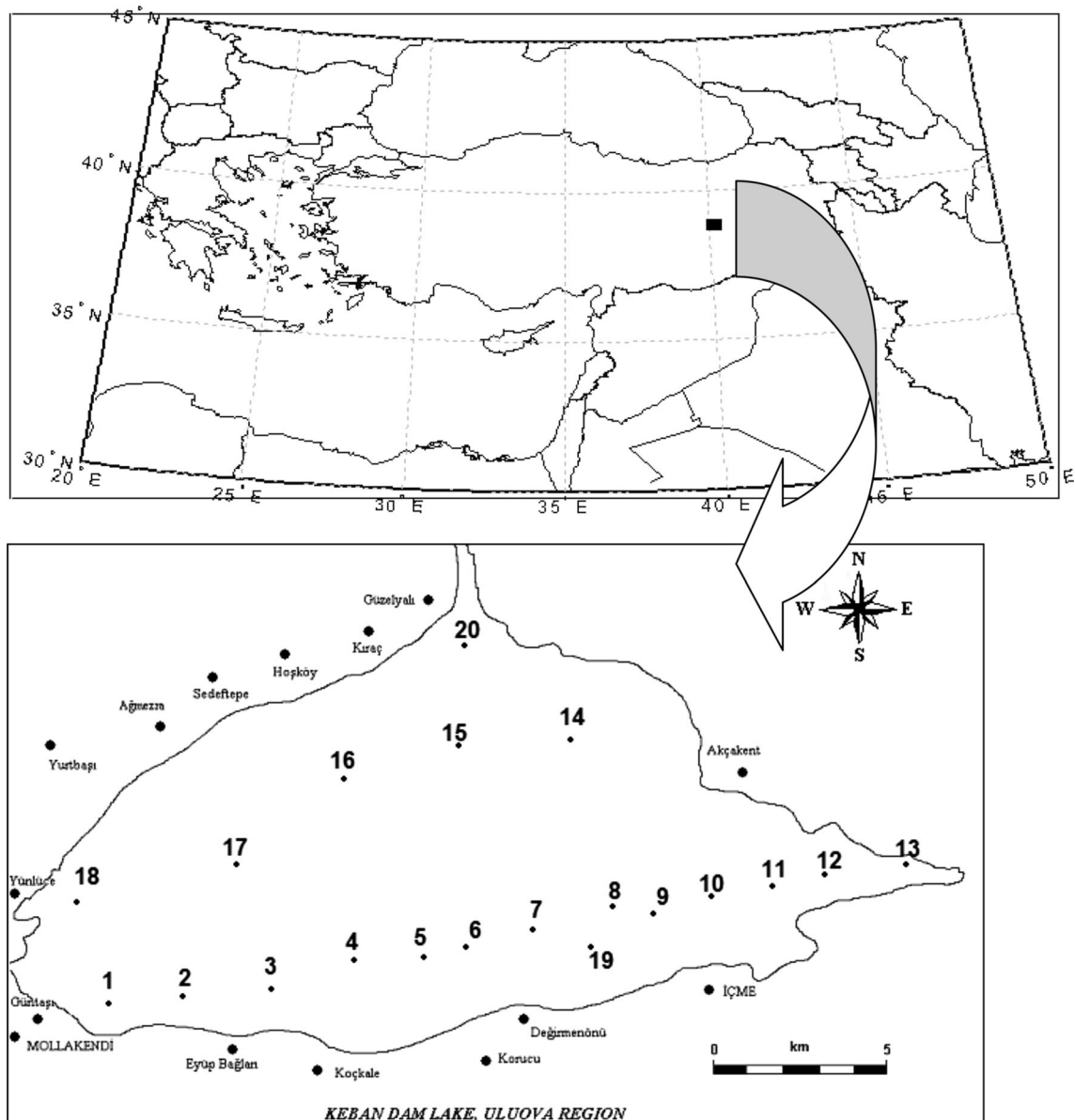
Springer

Fig. 1 Keban Dam and the sampling points

surface layer mineral content provides extra information about the existence of such elements and their distribution in the sediment under lakes.

In this study, the risk levels and distributions of major cations in a lake are estimated using stochastic risk analysis and spatial methodologies (Kim et al. 2016; Xue et al. 2015; Mor et al. 2006). Keban Reservoir is chosen as a pilot area for the proposed method due to its geological and geographical diversity, and applications of the methodologies are carried out on its reservoir lake. A risk assessment formulation is presented for the concentrations obtained from cation field measurements. Risk levels for different cations are presented through Weibull, lognormal and exponential models, and the theoretical probability

distribution function (pdf) and cumulative distribution function (cdf) of each cation measurement location are obtained. In addition, the spatial and transport characterisations of the cations are established using two-dimensional iso-curves created using the Kriging methodology (You et al. 2016; Külahcı and Şen 2009; Matheron 1963).

Experimental

Study area and water sampling

The Keban Dam Lake is the second largest freshwater body in Turkey. The study area (Uluova Region of Keban

Table 1 Basic data for Keban Dam

Station	Longitude (east, $x°.x'.x''$)	Latitude (north, $x°.x'.x''$)	Surface water (ppm)					Deep sediment (ppm)				
			Mg	Ca	K	Na	Zn	Mg	Ca	K	Na	Zn
1	39.25.27	38.36.39	110.80	31.20	5.10	28.92	1.85	64,925	12,460	45,812	58,751	39,393
2	39.26.39	38.36.48	103.00	30.70	5.05	31.80	2.02	12,247	91,340	14,951	50,571	53,193
3	39.27.18	38.36.53	108.60	27.01	5.00	26.80	4.72	10,531	98,888	10,581	53,481	45,063
4	39.27.58	38.37.01	108.60	32.89	5.00	27.20	7.84	13,652	10,827	12,581	34,101	58,213
5	39.28.22	38.37.16	115.30	33.73	5.00	35.70	1.90	12,391	11,077	10,768	59,311	36,343
6	39.28.56	38.37.25	103.90	30.37	4.95	27.20	1.70	11,763	10,327	12,881	63,131	59,413
7	39.29.29	38.37.42	103.20	36.20	5.10	24.20	1.63	14,833	96,011	94,312	65,171	56,711
8	39.31.06	38.38.08	102.19	33.73	5.15	26.30	1.60	13,430	96,651	16,453	67,351	40,503
9	39.31.53	38.38.02	110.80	34.15	5.10	35.60	1.60	11,813	97,707	84,412	53,271	65,921
10	39.32.40	38.38.24	110.39	48.44	5.10	34.00	4.16	14,825	10,887	62,882	60,784	59,673
11	39.33.28	38.38.38	105.64	31.20	5.05	24.70	1.94	12,150	88,912	11,271	54,581	31,323
12	39.34.04	38.38.48	93.76	28.60	5.20	25.60	5.03	12,402	80,404	26,802	28,801	21,743
13	39.34.48	38.39.10	94.41	27.01	5.05	26.40	1.72	41,468	10,598	89,062	59,831	35,033
14	39.32.42	38.39.52	93.55	29.95	5.00	36.50	1.50	22,317	87,995	13,587	66,411	32,173
15	39.31.28	38.39.35	108.23	28.20	5.05	28.90	1.85	14,569	81,061	89,428	35,451	12,263
16	39.30.20	38.39.10	103.91	32.41	5.25	26.40	1.58	31,034	88,834	20,581	55,711	33,513
17	39.27.41	38.38.15	100.03	29.95	5.15	25.50	3.67	71,124	77,215	17,421	56,941	33,763
18	39.24.54	38.37.58	112.30	28.20	5.10	29.70	2.92	73,304	94,822	58,112	58,121	31,703
19	39.31.23	38.37.19	100.46	29.10	5.15	29.70	3.01	57,349	84,783	84,062	63,681	23,863
20	39.29.40	38.40.45	106.51	30.70	5.00	31.10	1.75	15,299	10,693	86,472	65,391	32,763

Table 2 Theoretical distribution of independent process returns periods as a function of the average return period T

Average return period	Actual return period T_r exceeded various percentages of time or distance $P(T_r \geq j)$						
T	0.01	0.05	0.25	0.5	0.75	0.95	0.99
2	7.64	5.32	3	2	1.41	1.07	1.01
5	21.64	14.42	7.21	4.1	2.28	1.23	1.04
10	44.71	28.43	14.16	7.58	3.73	1.48	1.09
30	136.84	89.36	41.89	21.44	9.48	2.51	1.29
100	459.21	299.07	138.93	69.97	29.62	6.1	2
1000	4603.86	2995.23	1386.60	692.8	288.53	52.53	11.11

Reservoir) is approximately 150 km². It is situated at latitude 38°5′N and longitude 38°4′E, with an elevation of 1134 m above mean sea level. Surface water and deep sediment samples were taken at 20 stations in April and May 2011 in the geographic locations shown in Fig. 1. In particular, residential areas on the southern side of the lake contribute to the lake and the stations are arranged as in Fig. 1.

According to the observation values between 1937 and 1987, the average annual atmospheric temperature is 13.4 °C. Monthly average temperatures vary between −0.1 and 27.1 °C. The seasonal temperature of the lake changes between 2 and 35 °C.

The bottom of the lake is covered with clay, and the annual amount is estimated to be approximately 40,000 tonnes of silt and clay. The total hardness (TH), electrical conductivity (EC) and pH values of water are also calculated. The experimental procedures are performed three times for each station, and the standard deviations are calculated for about 10 %. Accordingly, TH, EC and pH values for all stations are measured as 191.73 mgCaCO$_3$/L, 343.91 μmho/cm and 8, respectively. pH measurements are performed with Orion (230) digital pH meter, and the electrical conductivities are measured with Jenway (4070) digital conductivity meter. The total

Table 3 Summary statistics for basic data

	Surface water (ppm)					Deep sediment (ppm)				
	Mg	Ca	K	Na	Zn	Mg	Ca	K	Na	Zn
Minimum	93.55	27.01	4.95	24.2	1.5	10,531	10,327	10,581	28,801	12,263
Maximum	115.3	48.44	5.25	36.5	7.84	73,304	98,888	94,312	67,351	65,921
Mean	104.7	31.68	5.07	29.11	2.7	26,571	62,074	43,121	55,542	40,128
Median	104.7	30.7	5.07	28.05	1.87	14,697	82,922	23,691	58,436	35,688
Standard error of mean	1.38	1.04	0.017	0.86	0.36	4931	8694.6	7528	2440	3238
Average deviation	4.93	2.97	0.06	3.12	1.24	17,977	35,765	30,646	7853	11,766
Standard deviation	6.18	4.65	0.07	3.84	1.64	22,056	38,883	33,668	10,915	14,485
Coefficient of variation %	5.9	14.6	1.5	13.0	60.0	83.0	62.6	78.0	19.0	36.0
Coefficient of skew	−0.426	2.594	0.474	0.748	1.952	1.343	−0.611	0.468	−1.401	0.184
Coefficient of kurtosis	−0.435	8.861	−0.149	−0.62	3.989	0.21	−1.71	−1.685	1.28	−0.67

hardness determinations are carried out using the titration system by titrimetric methods.

Surface water samples were taken at 25 cm depth and stored in 2-L polyethylene bottles for subsequent preparation and analysis. The bottles were rinsed at least three times with double-distilled water and 1:1 HNO_3/H_2O prior to sample collection (Özmen et al. 2004). Water samples were then passed through Whatman glass microfibre filters (GF/C) and acidified with (0.2 v/v) ultra-pure nitric acid (E. Merk, Darmstadt, Germany) to pH < 2 to minimise the absorption of metals onto the walls of the containers. Samples were stored at approximately 4 °C. Twenty sediment samples were collected using a stainless steel dredge. Sampling depth varied between 30 and 35 m. The sediment samples were placed in polyethylene bags and stored at 4 °C during their transport to the laboratory. They were then dried in an oven at 50 °C for 48 h. Approximately 200 mg of each sample was digested with HNO_3, HF and H_2O_2 in a Teflon bomb. Among the major elements measured in the water and sediment samples were Zn (Shimadzu AA-660 Model AAS), Ca, Mg, Na and K (Eppendorf Model AES). The concentrations of each element in both water and sediment samples are shown in Table 1. The measurements are performed three times with the standard deviation of about 10 % according to the reference materials proposed by NIST (Clesceri et al. 1989).

Theoretical methodology

Risk analysis

The simple risk, R, can be defined as the probability that the concentration of a major cation, X, will exceed a chosen major cation threshold, Q, at least once during a certain time duration, T, or over an area, A. In this study, the area will be defined by the number of sampling points, n, for a given major cation. If the sequence of future likely occurrences of X is $X_1, X_2,\ldots, X_n$, then the joint probability of non-occurrence, N, is defined according to Şen (1976, 1991, 1999) as:

$$N = P(X \leq Q) = P(X_1 \leq Q, X_2 \leq Q, \ldots, X_n \leq Q) \quad (1)$$

Hence, the simple risk, R, as a complementary event, is defined as:

$$R = 1 - P(X_1 \leq Q, X_2 \leq Q, \ldots, X_n \leq Q) \quad (2)$$

In the risk assessment of any design project, it is necessary to first establish the frequency of design major cation occurrence, i.e. the return period, T, after which it is possible to determine the magnitude of the major cation on the basis of the most suitable pdf. The return period is defined as the average length of time over which Q will be exceeded once. The random variable T_r, which specifies the time or distance between any two successive exceedances of the selected major cation threshold, is referred to as the waiting time. Its distribution, in the case of independent discrete observations at intervals of $1.\Delta t$, is given by Feller (1967) as

$$P(T_r \geq j) = q^{j-1} \quad (3)$$

or

$$P(T_r = j) = pq^{j-1} \quad (4)$$

where j is the discrete duration of non-exceedance. Hence, the return period, which is the expected value of the waiting time, is found by

$$E(T_r) = T = \sum_{j=1}^{\infty} jP(T_r = j) = p \sum_{j=1}^{\infty} jq^{j-1} = \frac{1}{p} \quad (5)$$

where $p = P(x > Q)$, i.e. the probability of exceedance of the selected major cation threshold value. The return period cannot be less than one. The theoretical distribution of the return period is given by Eq. (3), the solution of which is presented in Table 2, which shows T_r as a function of $1 + \ln[P(T_r \geq j)] / \ln(1 - 1/T)$.

Table 2 shows that over a long period or distance, 25 % of the intervals between instances of major cation concentrations exceeding 100 are less than approximately 30 time (distance) units, while an equal number are expected to be in excess of approximately 139 time (distance) units. In other words, to ensure 75 % safety that the desired threshold level will not be exceeded by a major cation within the next 30 time or distance units, the system must be designed for non-exceedance over 100 time (or distance) units.

The risk of overtopping a given major cation threshold can be obtained in terms of the return period using Eq. (2), which leads to

$$R = 1 - \left(1 - \frac{1}{T}\right)^n \quad (6)$$

Conversely, the risk can also be computed in terms of the rank and number of samples using Eq. (7)

$$R = \frac{m}{n+1} \quad (7)$$

where m is the rank and n is the number of samples.

Probability and cumulative distribution functions for distribution characterisations of major cations

The major cations (Mg, Ca, K, Na and Zn) in the Keban Dam Lake are described here by three different pdfs and cdfs: the lognormal, Weibull and exponential distribution functions. The distribution functions were computed using Eqs. 8–13.

Lognormal distribution

The lognormal pdf for $x > 0$ is given by Eq. 8. In a lognormal distribution, the parameters denoted μ and σ are, respectively, the mean (for a given location) and the standard deviation (scale).

$$f(x|\mu, \sigma) = \left(\frac{1}{x \ln(\sigma)\sqrt{2\pi}}\right) \exp\left(-\frac{(\ln(x) - \ln(\mu))^2}{2\ln(\sigma)^2}\right) \quad (8)$$

The cdf for the lognormal distribution is given by Eq. 9

$$F(x|\mu, \sigma) = \frac{1}{\ln(\sigma)\sqrt{2\pi}} \int_0^x \frac{\exp\left(-\frac{(\ln(t) - \ln(\mu))^2}{2\ln(\sigma)^2}\right)}{t} \, dt \quad (9)$$

Weibull distribution

For the $x \geq 0$ Weibull pdf, the α shape parameter and the β scale parameter are given by Eq. 10

$$f(x|\alpha, \beta) = \alpha\beta^{-\alpha} x^{\alpha-1} \exp\left(-\left(\frac{x}{\beta}\right)^\alpha\right) \quad (10)$$

The Weibull cdf is also given by Eq. 11

$$F(x|\alpha, \beta) = 1 - \exp\left(-\left(\frac{x}{\beta}\right)^\alpha\right) \quad (11)$$

Exponential distribution

The pdf of an exponential distribution is

$$f(x) = \lambda e^{-\lambda x} \quad (12)$$

The cdf is given by

$$F(x) = 1 - \lambda e^{-\lambda x} \quad (13)$$

Table 4 Correlation coefficients matrix

	Mg	Ca	K	Na	Zn	Mg[a]	Ca[a]	K[a]	Na[a]	Zn[a]
Mg	1									
Ca	0.338	1								
K	−0.238	0.114	1							
Na	0.298	0.306	−0.303	1						
Zn	0.059	0.081	−0.014	−0.200	1					
Mg[a]	−0.043	−0.278	0.364	−0.132	−0.031	1				
Ca[a]	−0.223	−0.258	0.442	−0.166	−0.155	0.019	1			
K[a]	0.045	0.098	0.111	0.084	−0.265	0.170	−0.052	1		
Na[a]	−0.004	0.214	−0.108	0.205	−0.599	0.222	−0.065	0.125	1	
Zn[a]	0.301	0.546	−0.273	0.174	0.141	−0.331	−0.207	−0.082	0.196	1

[a] Deep sediments

Results and discussion

Summary statistics for each cation are presented in Table 3. There are significant differences between the surface water and deep sediment cation concentrations. The following conclusions can be deduced from this table.

1. Comparison of the median and mean values indicates the skewness of the available data. If the median and mean values of any element are equal within ± 5 % limits, then this element has a symmetric pdf; otherwise, the pdf is asymmetric. On this basis, although the surface water data for Mg^{++}, Ca^{++}, K^+ and Na^+ have symmetric distributions similar to the normal pdf, the deep sediment data have asymmetric pdfs. This discrepancy represents one of the most significant differences between the surface and deep sediment results.

2. The skewness coefficient of Zn in surface waters is greater than 1, which implies that it does not abide with a normal distribution. On the other hand, Zn in bottom sediments has positive range as shown in Table 3. Accordingly, Zn distributions in the bottom sediments conform to the normal distribution.

3. The deep sediment cation concentrations have comparatively greater values than the corresponding surface water concentrations, indicating that the cations studied here accumulate in the sediment in this reservoir.

4. The standard deviation estimates the average deviation around the arithmetic mean value; in other words, it is a measure of the spread of the probability distribution. If the standard deviation is large, the distribution of the data points is widespread, and if the standard deviation is small, then the risk associated with this element is also small. A large standard deviation indicates that the concentration values are unstable. In general, a large standard deviation is not required in the hydrochemical analysis of major cations because in such a case, hazardous materials are more difficult to control and may display many extreme values.

5. For surface water, the sequence of the concentration values of the cations surveyed, in decreasing order, is Mg > Ca > Na > Zn > K. The Mg and Ca concentrations in surface water are greater than those of the other cations because the lake is rich in carbonate compounds. The order of the compounds in deep sediments is Ca > K > Mg > Zn > Na. Ca has the greatest concentration in the deep sediments, and, as mentioned in the introduction, it is the fifth most abundant element by mass in the Earth's crust. This element is enriched in limestone and dolomite in the form of $CaCO_3$ and in lime-free basic silicate rocks such as basalt (Merian et al. 2004a). The research area

is rich in $CaCO_3$. Ca is also more abundant in clay than other basic ions (Merian et al. 2004b). Na is not bound to clay minerals, as it has low bonding energy and so can be found both in the soil solution and in water. Na concentration is higher in saline soils and waters. There is fresh water in the research area; especially Na in the bottom sediments is ranked as the last in terms of the variables of interest. Distribution of the Zn is very irregular. It is therefore difficult to make meaningful interpretations about Zn. In this study, the main element affecting the distribution of Zn is clay in bottom sediments. Zn is easily absorbed by clay minerals (Viets 1962). On the other hand, K is also enriched in the clay minerals. K in the bottom sediments has a high concentration according to other elements. However, it has low concentration in the surface waters. The amount of K is transported from deep sediments towards the surface water, and one can say that it is of relatively small rates. Transport of the Mg in the water is comparatively more than other elements.

6. The coefficient of variation (CV) is the standard deviation divided by the mean, and it is a dimensionless measure of variation. This index allows comparison between various compounds even when their original units are different. A higher CV indicates greater dispersion of the variable, and a small CV implies smaller residuals attached to the prediction values. The CV plays a similar role as other measures of spread in experimental data, including the standard deviation or root mean squared residuals (SAS 2007). Of the various cations listed in the table, the CV of the surface water concentration of Zn is the highest, though Zn has the lowest mean concentration. This result implies that the Zn concentration has the most irregular variability of any of the cations measured in the surface water, and its variability is even greater than that of any element in the deep sediment. In the surface water, the cations in the order of decreasing CV are Zn > Ca > Na > Mg > K. According to these findings, the measurements of Zn in surface waters have a wider range than those of the other cations. Depending on the proximity of the sampling location to various sources, the main source of Zn in the surface water may be a smelter, a power station discharge, fertiliser production, vegetation or motor tyre wear (Swaine 2000). The Zn reserves in the basin are designated by the Turkey General Directorate of Mineral Research and Exploration (MTA 2011).

7. In deep sediments, the cations in the order of decreasing CV are Mg > K > Ca > Zn > Na. The basin of the Keban Dam contains magmatic and metamorphic rocks (e.g. basalt), both of which have a

Table 5 One-way ANOVA for the major cations

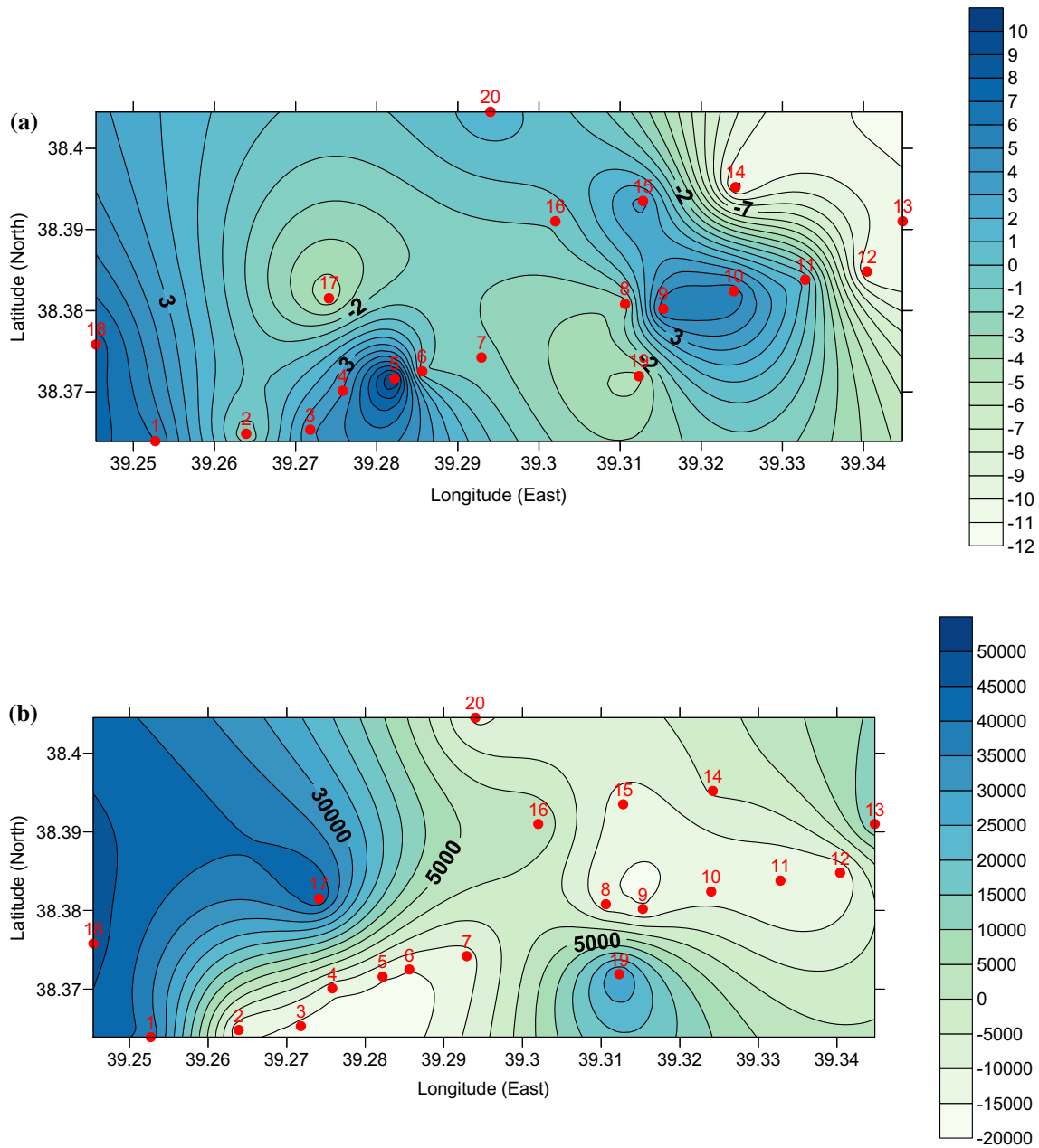| Source of variation	SS	df	MS	F	P value	F_{crit}
Between groups	1.186E+11	9	13,185,096,621	38.097	4.817E−38	1.929
Within groups	65,757,573,746	190	346,092,493.4			
Total	1.844E+11	199				

Fig. 2 Contour curves of deviations from the areal arithmetic means for Mg. **a** Surface water, **b** deep sediment

high Mg content. Mg-laden mineral, rock or soil particles may be transported into the lake floor by soil and wind erosion, increasing the Mg CV in deep sediments. Na has the smallest CV in the deep

sediments. Similarly, Mg in deep sediments has a wider quantity range in comparison to other cations.

8. Kurtosis is a measure of the sharpness of the pdf peak. Any symmetric pdf, such as the normal (Gaussian) pdf,
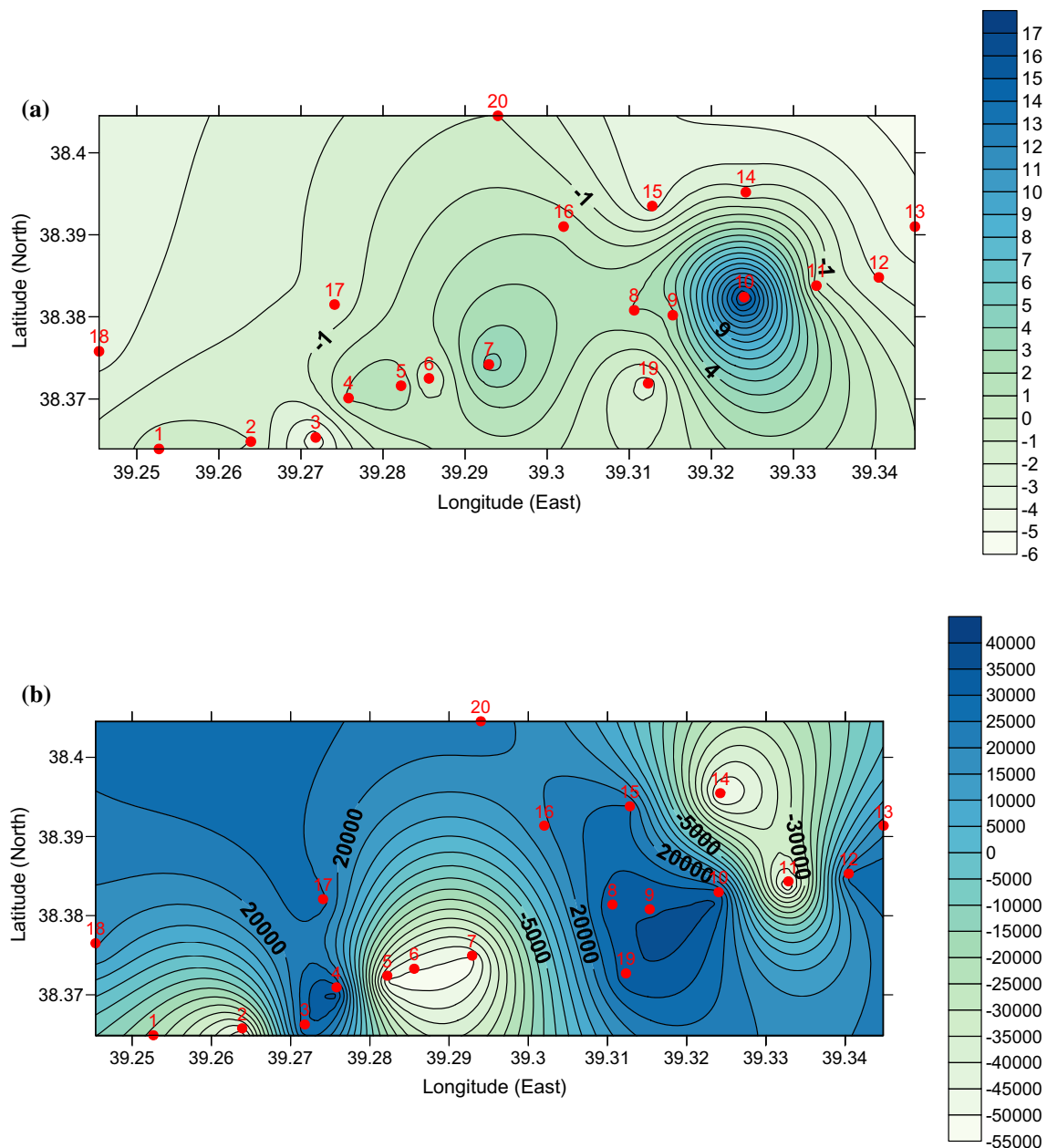
Fig. 3 Contour curves of deviations from the areal arithmetic means for Ca. **a** Surface water, **b** deep sediment

has a kurtosis value equal to zero. An increase in the kurtosis value implies a sharper pdf (Golden Software 2009). In surface water, Ca and Zn have positive coefficients of kurtosis (CK), as do Mg and Na in deep sediment. Mg, K and Na in surface water and Ca, K and Zn in deep sediments have negative CK values with a flat pdf, i.e. small kurtosis values.

The Ca and Zn in the surface water and Ca, K and Na in the bottom sediments are outside of the range, $(-1, +1)$, and therefore, the concentration values of these elements do not fit the normal distribution. This result indicates to their non-homogeneous distributions in the lake.

9. The coefficient of skewness (CS) is a measure of asymmetry in the pdf. A positive skew indicates a longer tail to the right, while a negative skew indicates a longer tail to the left. A perfectly symmetric distribution, such as the normal distribution, has a skew equal to zero (Golden Software 2009). Among the surface water cation concentrations, that of K has a CS closest to zero. This finding implies that K is homogeneously distributed in surface waters. Ca, K, Na and Zn have positive CS, indicating that their concentration values tend to be higher than the arithmetic averages. However, Mg has a negative CS,
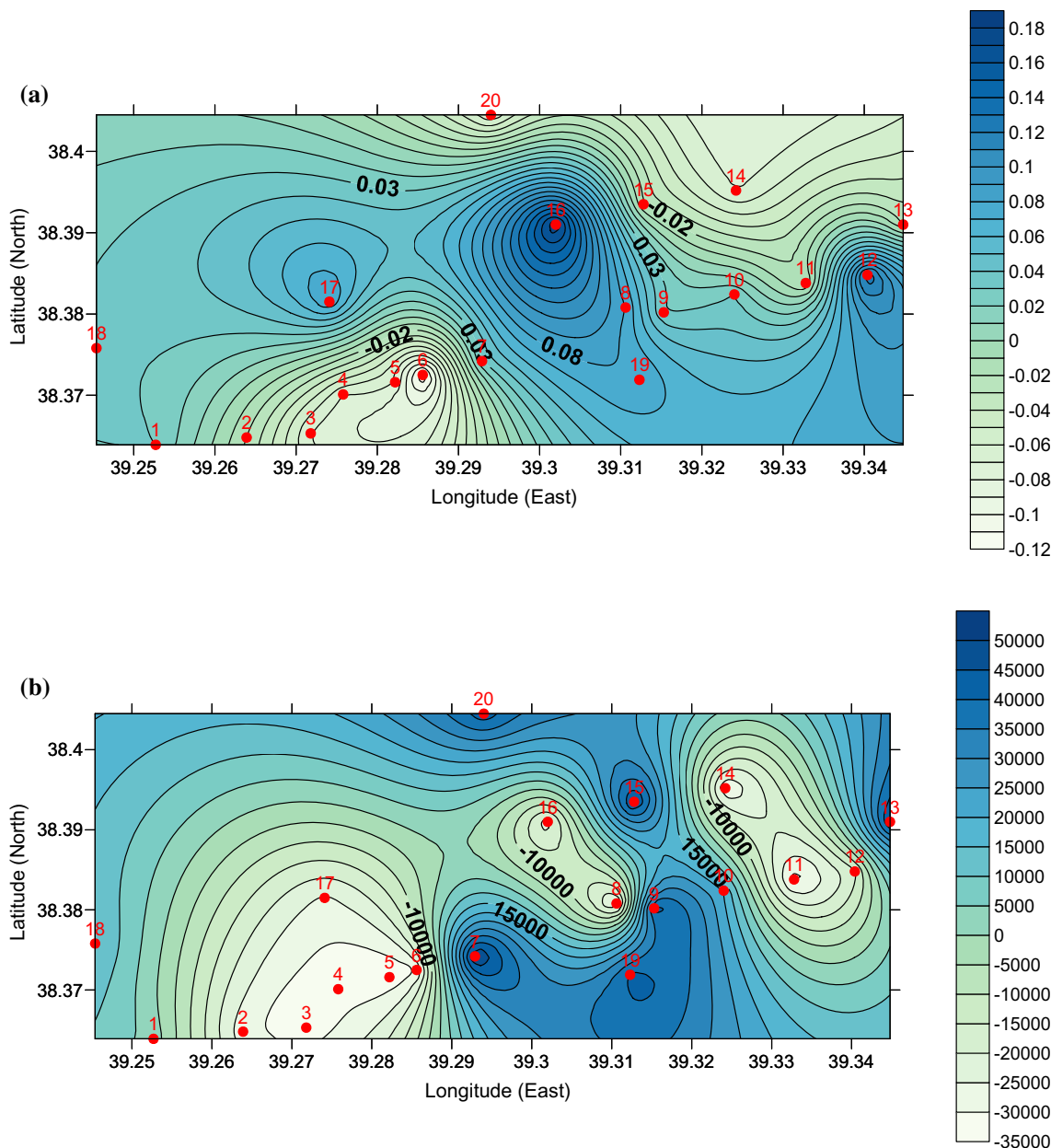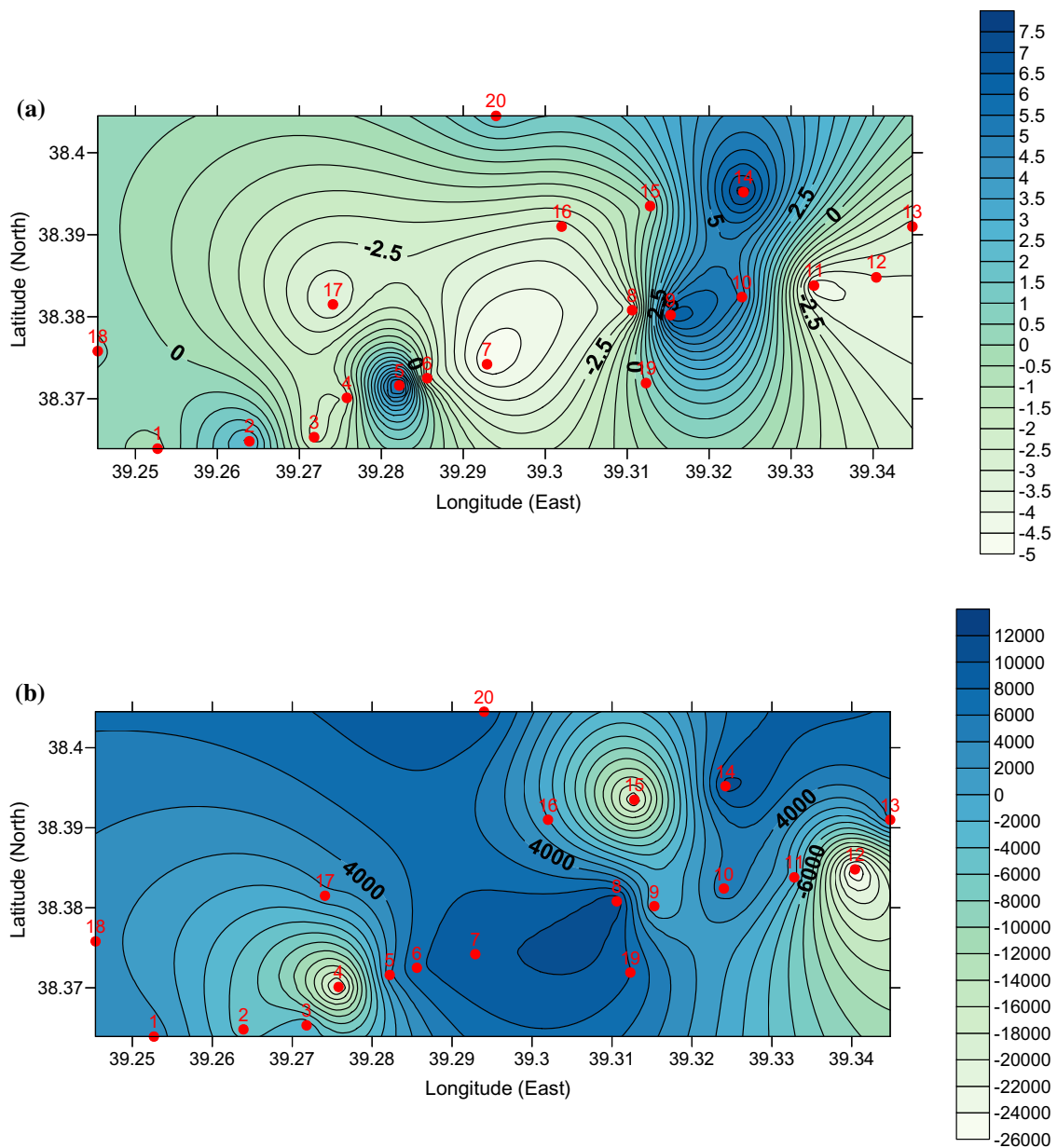
Fig. 4 Contour curves of deviations from the areal arithmetic means for K. **a** Surface water, **b** deep sediment

and its concentration values tend to be less than the average. Among the concentrations measured in the deep sediments, Mg, K and Zn have positive CS, whereas Ca and Na have negative values. The most symmetric pdf is that of Zn; its CS is close to 0. This result implies that Zn concentrations within the lake and in the deep sediments are in equilibrium.

Table 4 shows the correlation coefficient matrix between the surface water sediments and deep sediments.

There is a weak correlation between surface water sediments and deep sediments. The one-way ANOVA test

for these elements is shown in Table 5. The critical F value for the $\alpha = 0.05$ rejection region, denoted as F_{crit} in Table 5, corresponds to $F_{.05} = 1.92$. Thus, one can reject the null hypothesis that the ten means are equal if $F > F_{.05} = 1.92$ because the computed value of the test statistic, $F = 38.09$, is greater than the critical value.

The ANOVA analysis indicates that the means of the surface water concentrations are statistically different from those of the deep sediments. This finding is consistent with the correlation coefficient analysis shown in Table 4. That is, statistical analysis based on the given data indicates that

Fig. 5 Contour curves of deviations from the areal arithmetic means for Na. **a** Surface water, **b** deep sediment

there is no statistically significant correlation between the surface water concentrations and those in the deep sediments.

Spatial variation features: iso-cation curves

It is possible to represent the spatial distribution of each element separately using the Kriging methodology, originally suggested and developed by Krige (1951) and Matheron (1963), which is based on the concept of semivariogram and subsequent regionalisation of a given variable. This methodology maps regional features within the variation domain, which is the dam reservoir sample area in this study. The curve maps are prepared for deviations from the areal averages of each element, and one is thus able to identify deviations from the areal average concentration in addition to zonal patterns. Spatial distributions of the deviations are shown in Figs. 2, 3, 4, 5 and 6. In the following discussion, regions with greater or less than the zone value will be described as high or low regions, respectively.

The spatial analysis of Mg concentrations in surface waters reveals high zones at sample points 5, 9 and 10 and low zone at sample points 17 and 19, respectively (Fig. 2a).
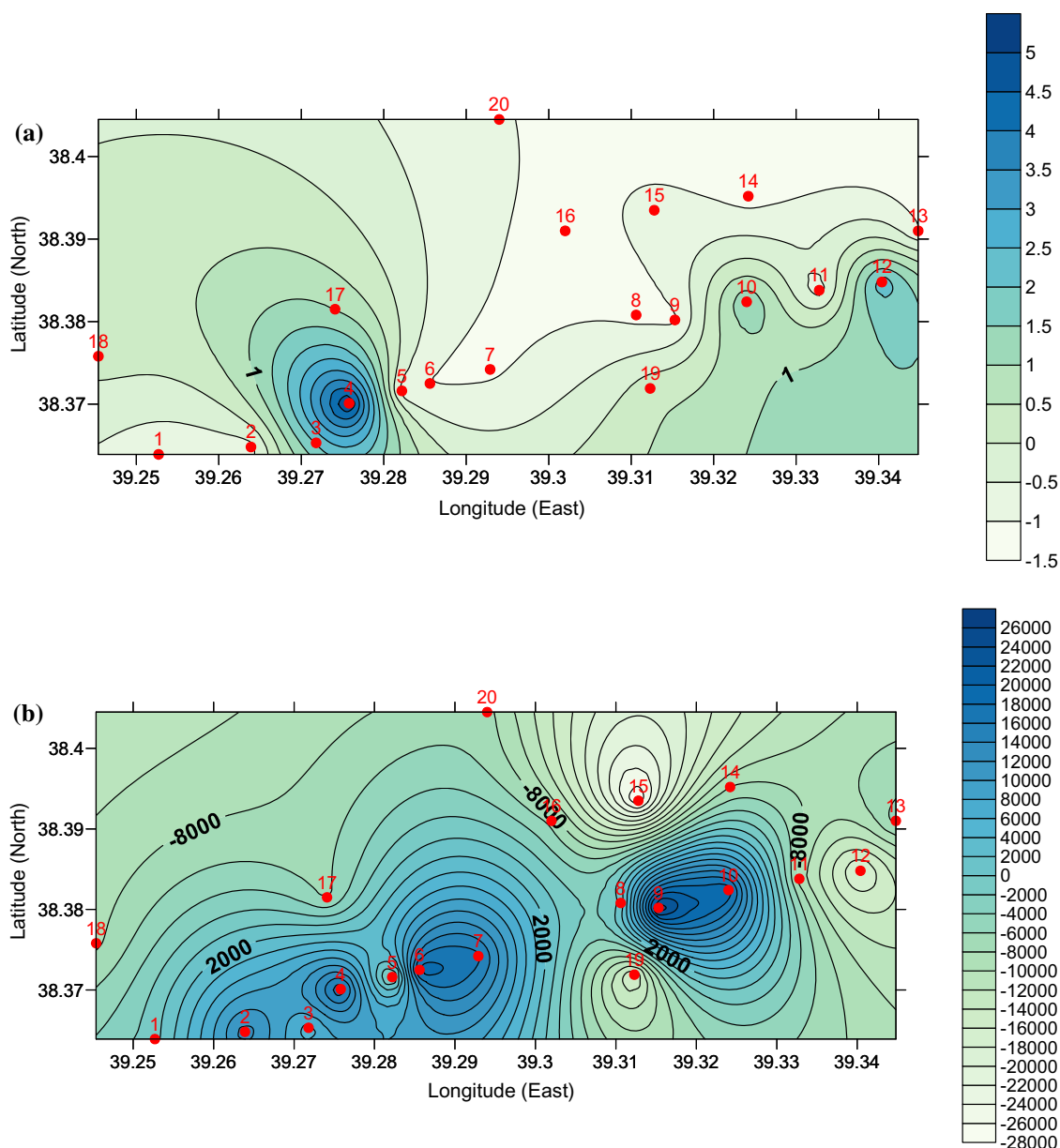
Fig. 6 Contour curves of deviations from the areal arithmetic means for Zn. **a** Surface water, **b** deep sediment

The high and low zones are adjacent. The existence of two zones of unusually high or low concentration is expected because water enters the reservoir from the centre, as in Fig. 1. Consequently, the flow is separated into two directions, east and west, and therefore, two vorticities form, causing regions of intensification (high zones) and dilution (low zones) in the Mg concentration. In the surface water domain, the high-concentration zone is on the west because the water outlet is in this direction. A high-concentration zone exists here due to the accumulation of stagnant water near the coastal area without any outlet.

Results for the deep sediment are shown in Fig. 2b. Due to the topography of the reservoir, Mg accumulates on the west coastal area, and there is also a minor high-concentration zone at the coastal area opposite to the entrance, which is due to low entrance velocity. In general, there is a low zone stretching from the south-west towards the outlet, which may imply an outlet on the east and groundwater recharge in the south-west low zonal area (Keban Dam Lake Limnological Study Report 1982).

In the surface water, the Ca concentration shows a dominant high zone around sample number 10, with a minor one at location 7 (Fig. 3a). This finding is attributable to the surface water entrance velocity, coupled with a current towards the outlet. There is a generally increasing trend in Ca concentrations in the surface water

from the west towards the outlet in the east. The Ca deep sediment concentrations, shown in Fig. 3b, also display spatial variation from the areal mean, with the same high-concentration zone observed in the surface water also appearing in the deep sediment. Additional Ca accumulation is also apparent in the north-western coastal area. The locations with low Ca concentrations might result from groundwater leakage from the bottom.

K concentrations in the surface waters are distributed more uniformly than either Ca or Mg (Fig. 4a); the data for K show relatively small concentrations throughout the reservoir volume. There is a sequence of high-K zones near the middle of the reservoir area, oriented from west to east, with the highest concentrations in the centre of the reservoir area. As with Ca and Mg, a low zone for K is observed at the south-west location; it may be due to groundwater seepage, minor surface water inflow or both.
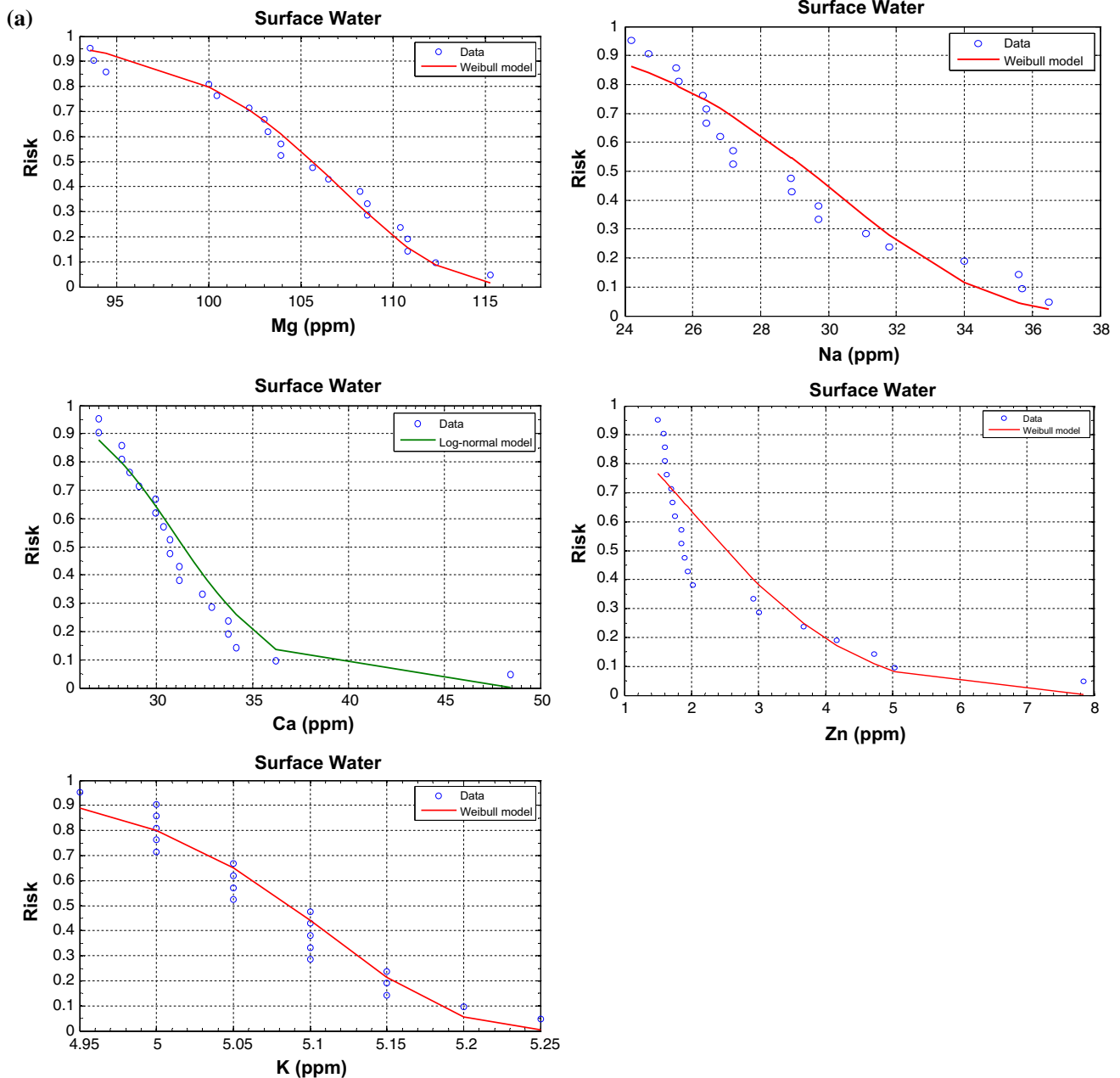
Fig. 7 a Fitted probability distribution functions for Mg, Ca, K, Na and Zn surface water cation measurements. The most appropriate pdfs for each cation were drawn using a MATLAB program written by the authors. **b** Fitted probability distribution functions for Mg, Ca, K, Na and Zn deep sediment cation measurements
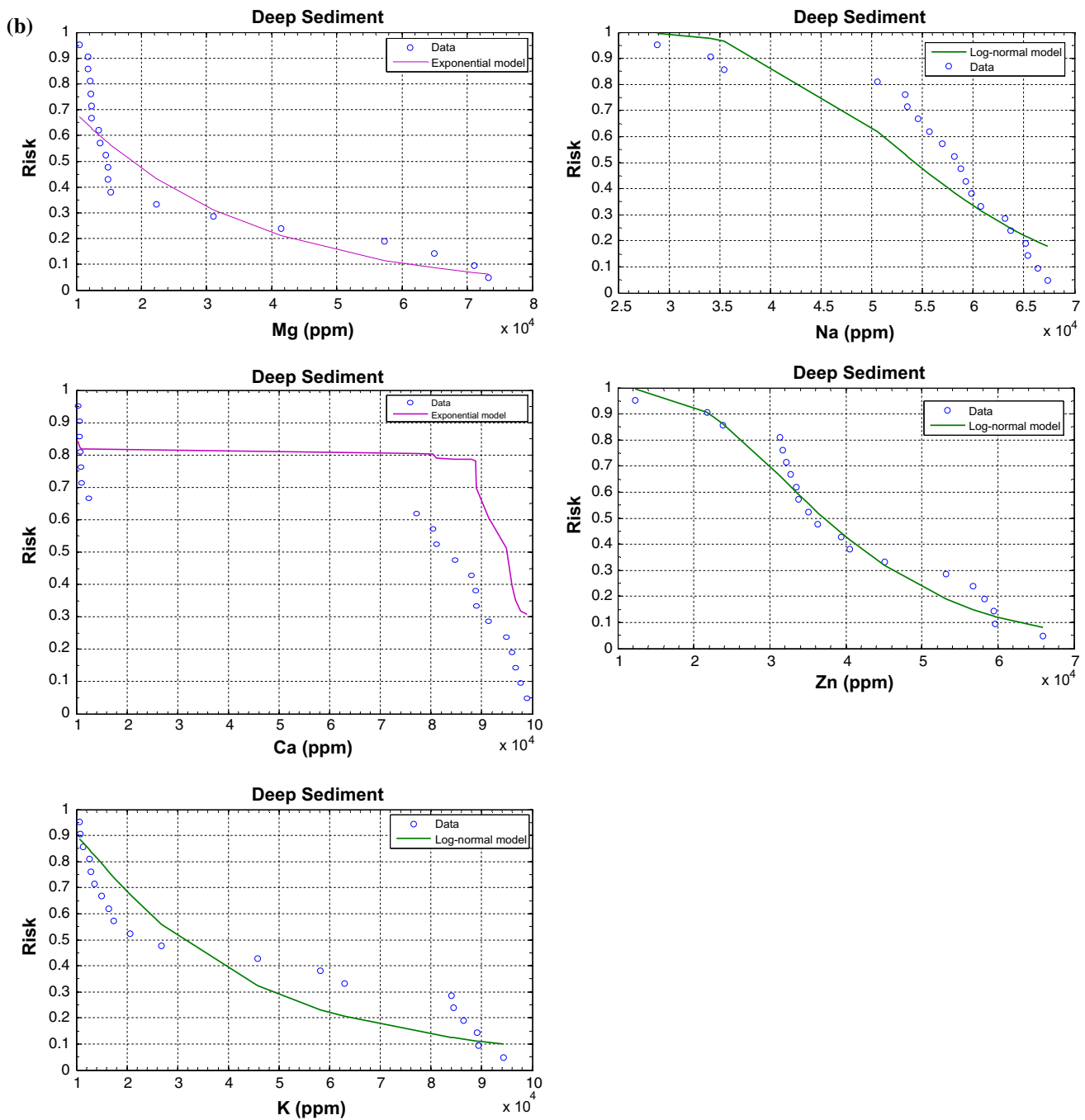
(b)

Fig. 7 continued

On the other hand, deep sediments have a different K accumulation pattern than the surface water. A very large low-concentration zone occurs near the south-western coastal area, suggesting steady groundwater flow or minor runoff contributions to this area (Fig. 4b).

The spatial variability of Na is shown in Fig. 5a for surface water concentrations; a belt of high concentration occurs on the east region of the lake and extends southeast. The rest of the reservoir shows low-Na concentrations

in the surface water. The deep sediment data vary greatly from the surface water values, showing very high accumulation concentrations with three low zones around sample locations 4, 8 and 14 (Fig. 5b).

The surface water Zn concentration data, shown in Fig. 6a, have an entirely different spatial pattern from all of the previous surface water maps. Its highest concentration zone lies near the south-western coastal area, opposite from the high-concentration zones for all of the previous

Table 6 Distribution function parameters of major cations in surface water

Surface water	Weibull		Lognormal	
	α	β	μ	σ
(a)				
Mg	107.53	20.56		
Ca			3.44	0.12
K	65.24	5.11		
Na	30.82	7.86		
Zn	3.06	1.84		

Deep sediment	Exponential	Lognormal	
	λ	μ	σ
(b)			
Mg	26,571		
Ca	62,075		
K		10.32	0.87
Na		10.9	0.23
Zn		10.52	0.40

elements. This result suggests that groundwater seepage or inland surface inflow in this area does not convey Zn. Zn seems to enter the lake only from the main entrance water and, as expected based on flow velocity direction and dispersion, there are two high zones, with the second occurring at the western coastal area south of the outlet point.

The deep sediment map in Fig. 6b shows high-concentration zones at the coastal areas opposite from the inlet point and their sequence covers sample locations starting from 2 and continuing towards the east, including sites 3–10. Almost all of the sites near the inlet and outlet points show low concentrations of Zn in the deep sediment layer.

Risk assessments

The surface water and the deep sediment concentrations of the cations shown in Table 1 are sorted from smallest to largest and ranked. The risk (R) and return period (T) are then computed using Eqs. 6 and 7, and the risk graphs for the data are shown in Fig. 7a, b. A MATLAB® program was written to find the most appropriate pdfs for the sample concentrations in Table 1. The lognormal, Weibull and exponential pdfs were calculated, and the α, β, μ, σ and λ parameters were obtained as shown in Table 6a, b. Equations 8–13 were used to calculate these parameters.

Figure 7a, b indicate the best-fit pdfs for each of the cations. Mg, K, Na and Zn concentrations in the surface water of the lake fitted best to the Weibull pdf, and only Ca concentrations in the surface water fitted best to the lognormal pdf (Table 6a). Mg and Ca concentrations in the deep sediments of the lake fitted best to the exponential pdf, and K, Na, and Zn concentrations in the deep sediments fitted best to the lognormal pdf (Table 6b).

The change in β's size is one of the most important aspects of the effect of β on the Weibull distribution. Weibull distributions with $\beta > 1$ have a failure rate that increases with time, also known as wear-out failure (Fig. 7; Külahcı 2011). The lognormal distribution is closely related to the normal distribution (Evans et al. 2000). Hence, the Ca concentrations in the surface water and the K, Na, and Zn concentrations in the deep sediments were dispersed more regularly than the other elements measured in the lake (Fig. 7a, b). The risk resulting from Mg and Ca concentrations in the deep sediments decreased exponentially (Fig. 7b).

The theoretical pdfs of the cations were determined using Eqs. 8, 10 and 12 and Table 6a, b. Figure 7a, b imply that high Mg, Ca, K, Na and Zn values occur rarely, whereas small values are abundant. The cumulative pdfs were obtained using Eqs. 9, 11 and 13, yielding Figs. 8a and 9a. These figures show the change in the probability of occurrence of concentrations less than any given threshold value on the horizontal axis. By definition, the probability of non-occurrence is a complementary value to the probability of occurrence, as apparent in Figs. 8b and 9b.

Conclusions

The distributional behaviours and the probabilities of occurrence and non-occurrence of major cations are very difficult to predict in a research area intended. Therefore, by taking advantage of spatial methodology in this study, iso-cation curves are suggested, which represent visually the distribution behaviours of the cations. In addition, the "return period" concept from the meteorology, climate and hydrology disciplines is adapted for the distribution behaviours of the cations and finally, the probabilities of presence or absence of the cations are calculated in an area. These calculations are very important to understand whether the cation concentrations cross a certain threshold level or not.

Iso-cation curves provide great benefits to understand how the distribution of cations comes into existence. Hence, cation transportation can be realised completely in the field of research. Such a situation is very significant for researchers in the fields of all environmental scientists and hydrologists as well as researchers in related fields. Likewise, estimation of the probability distribution of cations is of paramount importance for the prevention of environmental pollution.
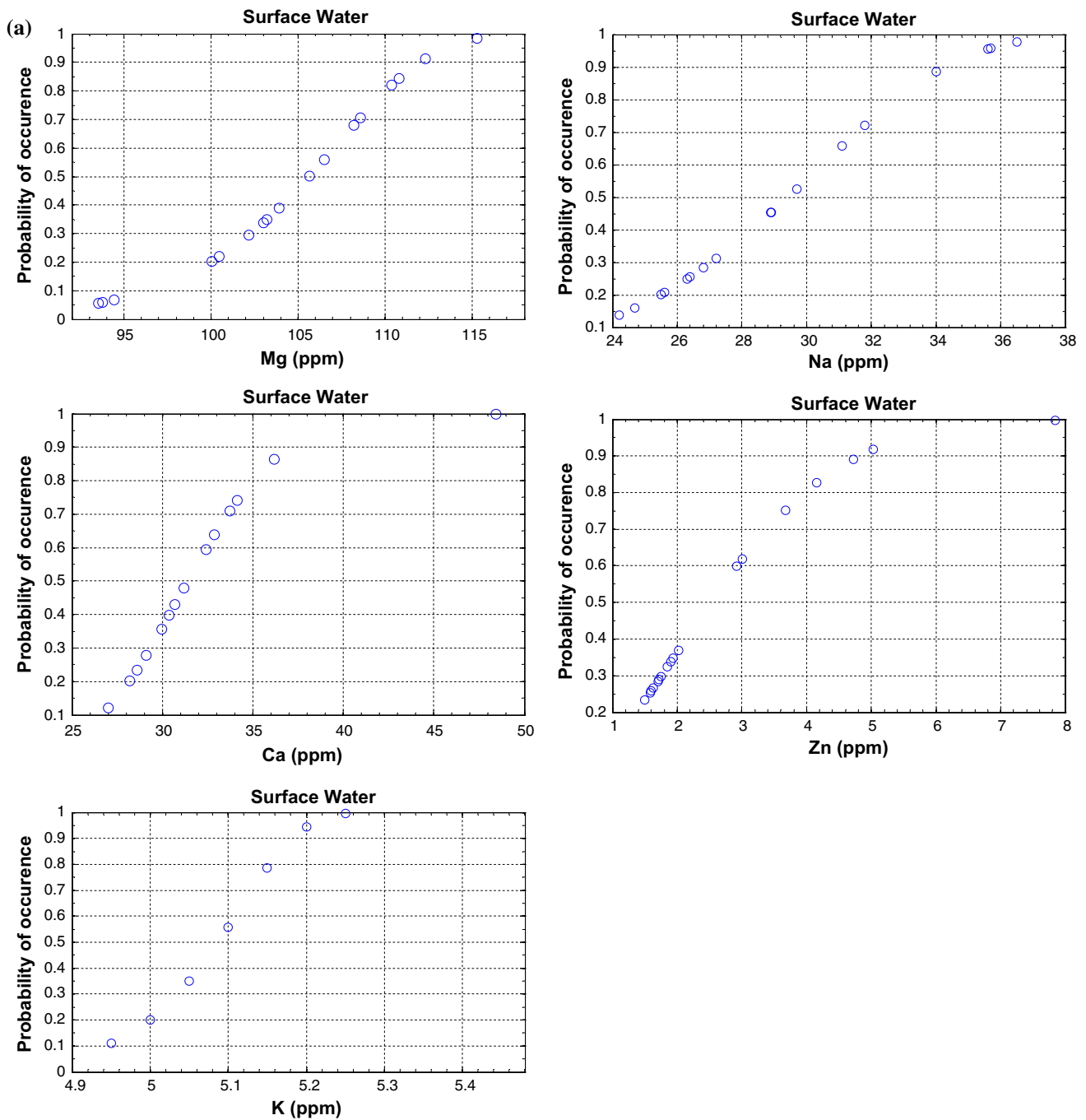
Fig. 8 a Cumulative pdf for major cations in surface water. **b** Probability of non-exceedence for major cations in surface water

The statistical parameters of the various elements are explained, and the patterns resulting from the spatial distributions of the elements are interpreted. The Kriging methodology of regionalisation is used to depict the spatial variation in cation concentration through a sequence of iso-cation maps, and stochastic risk analysis methodology applications to the data. Distribution models, specifically pdfs and cdfs, are used to assess the risk of any major cation concentration at a given location exceeding a threshold level.

The Kriging method is recommended in order to see the spatial distribution of cations, because this method provides significant contributions for interpretations.

Invariably and expectedly, the deep sediments have far greater cation concentrations than the surface waters, which are in a constant dynamic state due to water inflow and outflow. The high sediment concentrations are due to accumulation processes in the sediments. The cation concentrations in the bottom
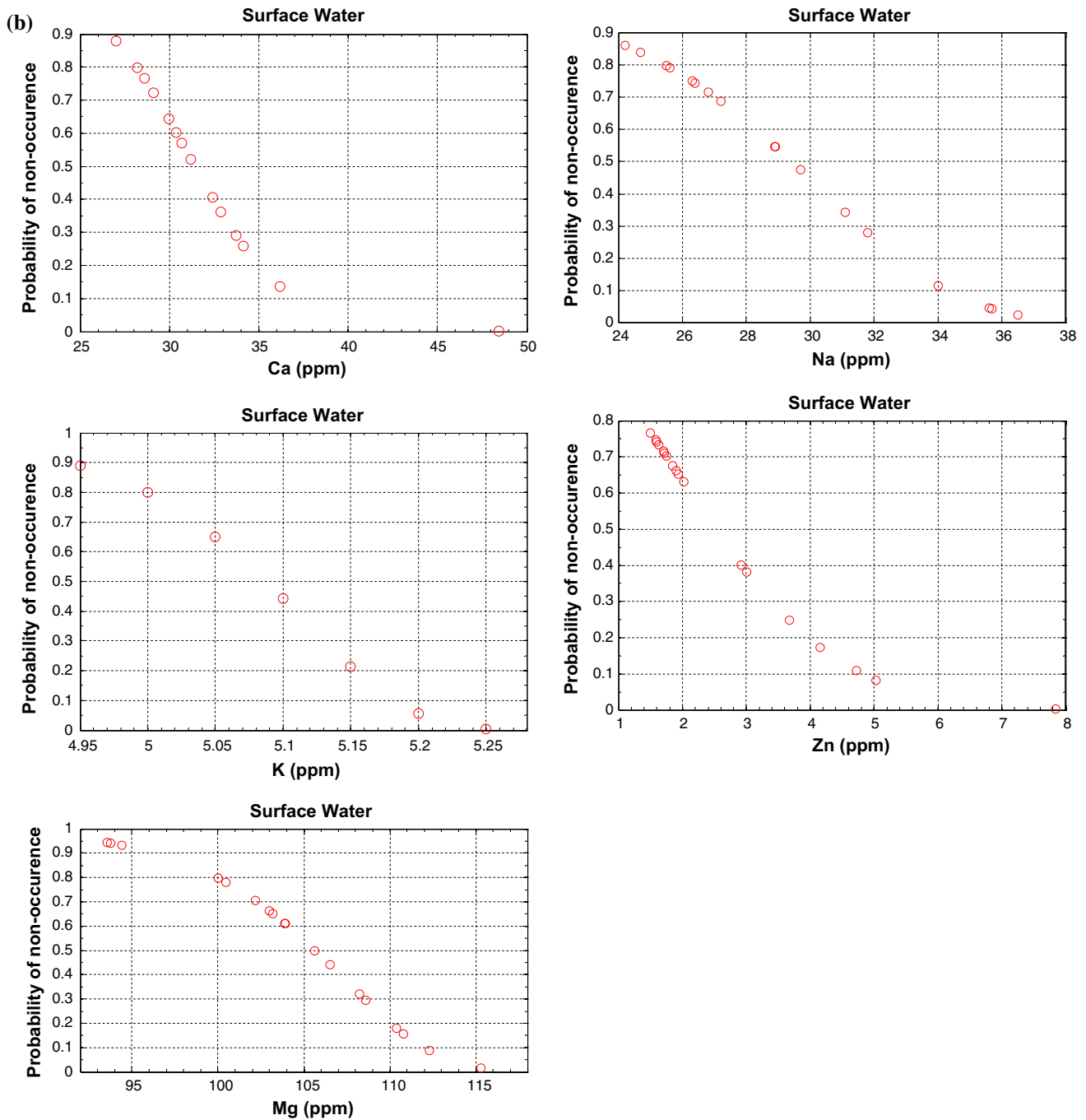
(b)

Fig. 8 continued

sediments tend to accumulate. One of the biggest causes of this phenomenon in the bottom of the lake is the coverages of clay, and the clay layers capture the cations.

The surface water element concentrations appear to result from dispersion and dilution processes, whereas the sediment concentrations of each element depend on the bottom topography, groundwater seepage or other minor land surface inflows into the reservoir.

Mg, K, Na and Zn cations in the surface water of the lake are fitted to the Weibull pdf, suggesting that the distribution of these cations in the lake has a randomness that increases with time. Ca concentrations in the surface water fit best to the lognormal pdf, as K, Na and Zn concentrations in the lake deep sediments. This result means that these cations have relatively regular distributions in the lake. Mg and Ca concentrations in the deep sediments decreased exponentially with time,

suggesting faster transport of Mg and Ca than other cations.

Mg and particularly Ca in both surface water and sediments in the bottom of some stations have high concentrations. These regions are rich in terms of limestone and dolomite.

According to the statistical calculations, Zn in surface waters and Na in bottom sediments are scattered over a wide area. The coefficient of variation (CV) to address this situation is a useful statistical tool.

Finally, as a result of this work, iso-cation curves and achievement of the probabilities of occurrence and/or non-
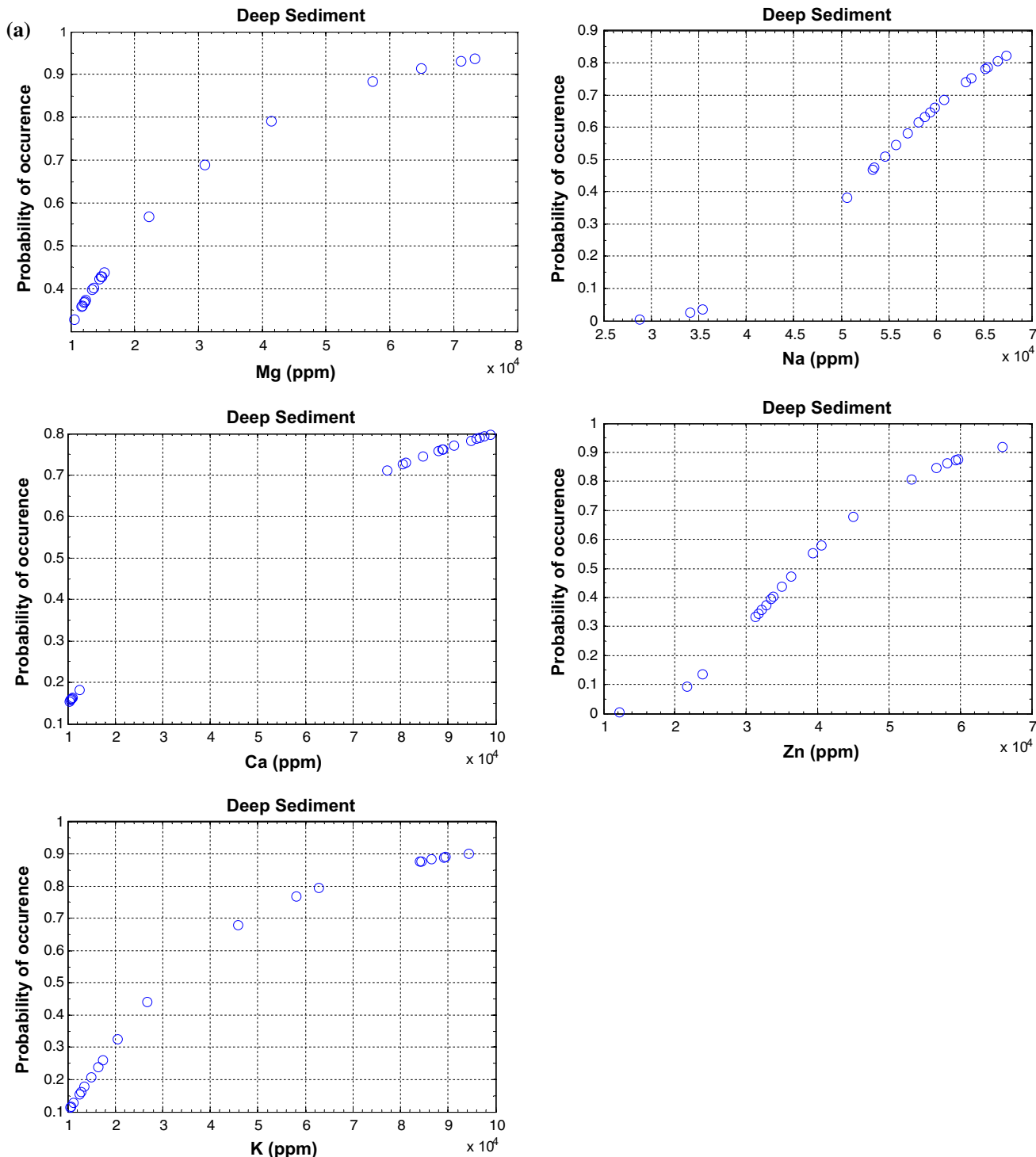
Fig. 9 **a** Cumulative pdf for major cations in the deep sediments. **b** Probability of non-exceedence for major cations in the deep sediments
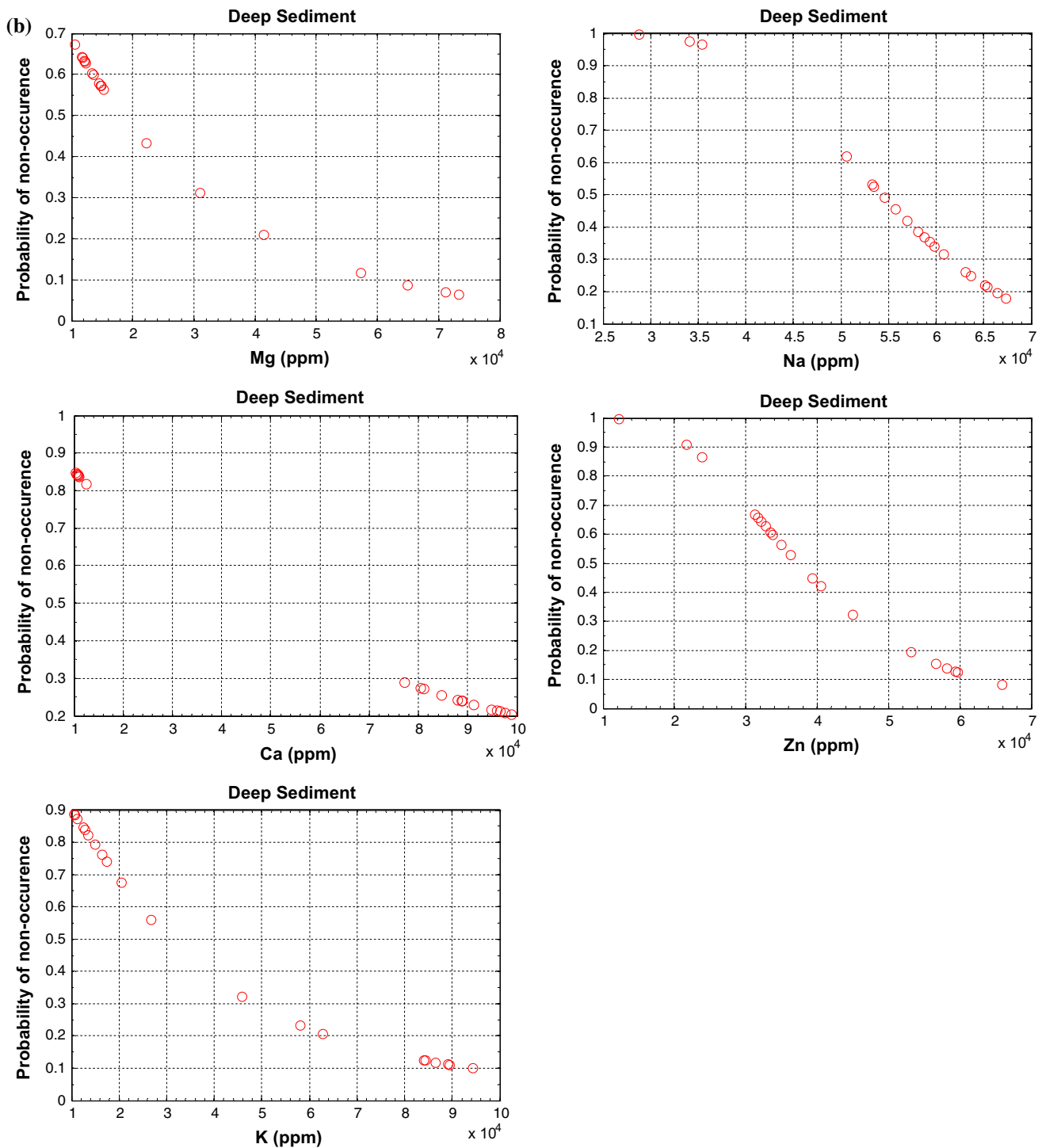
(b)

Fig. 9 continued

occurrence of cations in any research area can be generalised to all of the environment sciences. This calculation can be done not only for cations but also easily for all pollutants at micro- and macroscales.

References

Clesceri LS, Greenberg AE, Trussell RR (1989) Standart methods for the examination of water and wastewater. American Public Health Association, Washington, USA, Part 7000-7500

Evans M, Hastings N, Peacock B (2000) Statistical distributions, 3rd edn. Wiley, New York

Feller W (1967) An introduction to probability theory and its application, vol 1. Wiley, New York, p 509

Golden Software (2009) Grapher version 8.0.278. Golden, Colorado

Keban Dam Lake Limnological Study Report (1982) Ministry of Energy and Natural Resources, Operations and Maintenance Department, Ankara

Kim H-S, Chung C-K, Kim H-K (2016) Geo-spatial data integration for subsurface stratification of dam site with outlier analyses. Environ Earth Sci 75:168

Krige DG (1951) A statistical approach to some basic mine valuation problems on the Witwatersrand. J Chem Metall Min Soc S Afr 52:119–139

Külahcı F (2011) A risk analysis model for radioactive wastes. J Hazard Mater 191:349–355

Külahcı F, Şen Z (2009) Spatio-temporal modeling of ^{210}Pb transportation in lake environments. J Hazard Mater 65:525–532

Matheron G (1963) Principles of geostatistics. Econ Geol 58:1246–1266

Merian E, Anke M, Ihnat M, Stoeppler M (2004a) Elements and their compounds in the environment, vol 1. Wiley, Weinheim

Merian E, Anke M, Ihnat M, Stoeppler M (2004b) Elements and their compounds in the environment, vol 2. Wiley, Weinheim

Mor S, Ravindra K, Dahiya RP et al (2006) Leachate characterization and assessment of groundwater pollution near municipal solid waste landfill site. Environ Monit Assess 118:435–456

MTA (2011) http://www.mta.gov.tr/mta_web/maden/elazig.asp

Özmen H, Külahcı F, Çukurovalı A, Doğru M (2004) Concentrations of heavy metal and radioactivity in surface water and sediment of Hazar Lake (Elazığ, Turkey). Chemosphere 55:401–408

SAS (2007) UCLA: Academic Technology Services, Statistical Consulting Group. http://www.ats.ucla.edu/stat/sas/notes2/

Şen Z (1976) Wet and dry periods of annual flow series. ASCE J Hydraul Div 102:1503–1514

Şen Z (1991) Probabilistic modelling of crossing in small samples and application of runs to hydrology. J Hydrol 124:345–362

Şen Z (1999) Simple risk calculations in dependent hydrological series. J Hydrol Sci 44:871–878

Swaine DJ (2000) Why trace elements are important. Fuel Process Technol 65:21–33

Viets FG (1962) Chemistry and availability of micronutrients in soil. J Agric Food Chem 10:174–178

Xue Y, Meng X, Wasowsk J et al (2015) Spatial analysis of surface deformation distribution detected by persistent scatterer interferometry in Lanzhou Region, China. Environ Earth Sci 75:80

You M, Huang Y, Lu J, Li C (2016) Fractionation characterizations and environmental implications of heavy metal in soil from coal mine in Huainan, China. Environ Earth Sci 75:78